Natural-frequency Analysis of Laminated Composite Shell

E. Kormanikova

Abstract— The paper deals with a numerical approach of mode-frequency analysis of a simply-supported laminated doubly curved shell. For laminated shell the first-order shear deformation theory is capable of accurately predicting the shell behaviour. Transverse displacement field leads to using shear correction factor. Theory is also based on the assumption that the thickness to radius ratio of shell is small compared to unity and hence negligible. The governing equations are derived in orthogonal curvilinear coordinates and than these equations are rediced to those of doubly curved shell. Linear layered structural shell elements are used in FEM analysis. The natural frequencies of laminated orthotropic doubly curved shell with simply supported ends are solved. The numerical analysis is conducted to determine the effect of symmetry with respect to mid-plane, fibre orientation and width-to-thickness ratio to change of resonant frequencies.

Keywords— Vibration Analysis, Laminated Composite Shell, FEM analysis.

I. INTRODUCTION

Composite materials like fibre reinforced plastics are often used in fields like automotive, aerospace, and civil engineering [1,2,3]. Composites are most often used in lightweight structures where the laminated shells tend to be thin with respect to their in-plane extensions.

Layered shell models are used more and more in structural analysis with new material systems. The large amount of literature in this field indicates how many different problems and mechanical situations are addressed by shell analysis. Wung [4] presented a continuum-based shell element with transverse deformation. The element is based on first-order shear deformation theory (FSDT) and fourth-order transverse deformation. Whitney and Pagano [5] developed a Mindlin-type FSDT for multi-layered anisotropic plates. Similar classical laminate theory (CLT) and FSDTs are developed for multi-layered shells [6,7]. The free vibration investigation of simply supported sandwich plate is presented in [8]. The static and dynamic analyzes of single- and multi-layered plates and shells are investigated in [9-12]. Amabili and Reddy [13] worked on the use of higher order shear deformation nonlinear theory for shells of generic shape, taking geometric imperfections into account. They found that results were

Eva Kormanikova is with the Department of Structural Mechanics, Institute of Structural Engineering, The Technical University of Kosice, Faculty of Civil Engineering, Vysokoskolska 4, 042 00 Kosice, Slovak Republic (e-mail: eva.kormanikova@tuke.sk).

obtained by keeping non-linear terms of the Von Karman type for amplitudes of about two times the shell thickness.

II. ANALYTICAL ANALYSIS

Laminate shells can be also modelled as two-dimensional structural elements but with single or double curved reference surfaces (Fig. 1). Figure 1 shows a laminated doubly curved panel of rectangular platform, of total thickness h.

The coordinates x_1 and x_2 represents the directions of the lines of curvature of the middle surface, while the x_3 - axis is a straight line perpendicular to the middle surface (Fig. 2). R_i ($i=1, 2$) denotes the principal radii of curvature of the middle surface.

The displacement field, based on first-order shear deformation theory, is given by

$$u_1 = (1 + x_3 / R_1)\overline{u}_1 + x_3 \frac{\partial u_3}{\partial x_1}$$

$$u_2 = (1 + x_3 / R_2)\overline{u}_2 + x_3 \frac{\partial u_3}{\partial x_2}$$

$$u_3 = \overline{u}_3 \tag{1}$$

in which u_i ($i = 1, 2, 3$) represents the components of displacement at a point x_i ($i = 1,2,3$), while $\overline{u}_i$ denotes the same for the corresponding point at the mid-surface.

Assumptions of shallowness, vanishing geodesic curvatures, transverse inextensibility and the strain displacement relations for a double curved shell, based on first-order deformation theory, are given by

$$\varepsilon_1 = \overline{\varepsilon}_1 + x_3\kappa_1 \qquad \varepsilon_2 = \overline{\varepsilon}_2 + x_3\kappa_2 \qquad \varepsilon_4 = \overline{\varepsilon}_4$$

$$\varepsilon_5 = \overline{\varepsilon}_5 \qquad \varepsilon_6 = \overline{\varepsilon}_6 + x_3\kappa_6 \tag{2}$$

where

$$\overline{\varepsilon}_1 = \frac{\partial u_1}{\partial x_1} + \frac{u_3}{R_1} \qquad \overline{\varepsilon}_2 = \frac{\partial u_2}{\partial x_2} + \frac{u_3}{R_2} \qquad \overline{\varepsilon}_4 = \frac{\partial u_3}{\partial x_1} - \frac{u_1}{R_1}$$

$$\overline{\varepsilon}_5 = \frac{\partial u_3}{\partial x_2} - \frac{u_2}{R_2} \qquad \overline{\varepsilon}_6 = \frac{\partial u_2}{\partial x_1} + \frac{\partial u_1}{\partial x_2} \tag{3}$$

$$\kappa_1 = \frac{\partial^2 u_3}{\partial x_1^2} \qquad \kappa_2 = \frac{\partial^2 u_3}{\partial x_2^2}$$

$$\kappa_6 = 2\frac{\partial^2 u_3}{\partial x_1 \partial x_2} - \frac{1}{2}\left(\frac{1}{R_1} - \frac{1}{R_2}\right)\left(\frac{\partial u_2}{\partial x_1} - \frac{\partial u_1}{\partial x_2}\right) \tag{4}$$
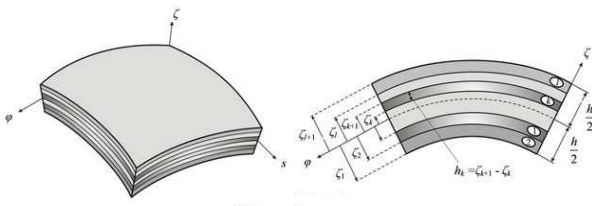
Fig. 1 Double curved laminated shell and layout of layers [11]

The curved shell geometry, illustrated in Figure 2 [14], is described by the coordinates (x_1, x_1, x_3) and it is subdivided into angular segments with the apex angles $d\varphi, d\vartheta$ and constant curvature radii of the centerline R_1 and R_2.
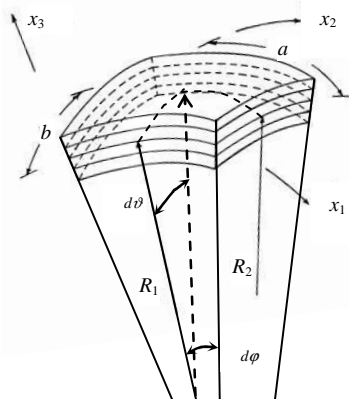

Fig. 2 Geometry of double curved laminated shell

It is assumed that the transverse normal stress is negligible in general, it is verified that σ_3 is small compared to τ_{13} and τ_{23}, except near the shell edges, so that the hypothesis is a good approximation of the actual behavior of moderately thick shells. The stress–strain relations for the n-th orthotropic lamina of the shell, in the material principal coordinates are obtained under the hypothesis $\sigma_3 = 0$,

$$\begin{Bmatrix} \sigma_1 \\ \sigma_2 \\ \sigma_4 \\ \sigma_5 \\ \sigma_6 \end{Bmatrix}^{(n)} = \begin{bmatrix} C_{11} & C_{12} & 0 & 0 & 0 \\ C_{21} & C_{22} & 0 & 0 & 0 \\ 0 & 0 & G_{23} & 0 & 0 \\ 0 & 0 & 0 & G_{13} & 0 \\ 0 & 0 & 0 & 0 & G_{12} \end{bmatrix}^{(n)} \begin{Bmatrix} \varepsilon_1 \\ \varepsilon_2 \\ \varepsilon_4 \\ \varepsilon_5 \\ \varepsilon_6 \end{Bmatrix} \tag{5}$$

where G_{23}, G_{13}, G_{12} are the shear moduli, the superscript (n) refers to the n-th layer within a laminate. Eq. (5) is obtained under the transverse isotrophy assumption with respect to planes orthogonal to axis 1, so that $E_1 = E_3$, $\nu_{12} = \nu_{13}$ and $G_{12} = G_{13}$.

The internal forces can be written in following form

$$\mathbf{N} = \begin{Bmatrix} N_1 \\ N_2 \\ N_6 \end{Bmatrix} \quad \mathbf{M} = \begin{Bmatrix} M_1 \\ M_2 \\ M_6 \end{Bmatrix} \quad \mathbf{V} = \begin{Bmatrix} V_1 \\ V_2 \end{Bmatrix} \tag{6}$$

where

$$N_1 = \int_{-\frac{h}{2}}^{+\frac{h}{2}} \sigma_1 dz \qquad M_1 = \int_{-\frac{h}{2}}^{+\frac{h}{2}} \sigma_1 z dz$$

$$N_2 = \int_{-\frac{h}{2}}^{+\frac{h}{2}} \sigma_2 dz \qquad M_2 = \int_{-\frac{h}{2}}^{+\frac{h}{2}} \sigma_2 z dz$$

$$N_6 = \int_{-\frac{h}{2}}^{+\frac{h}{2}} \tau_6 dz \qquad M_6 = \int_{-\frac{h}{2}}^{+\frac{h}{2}} \tau_6 z dz \tag{7}$$

$$V_1 = \int_{-\frac{h}{2}}^{+\frac{h}{2}} \tau_{xz} dz \qquad V_2 = \int_{-\frac{h}{2}}^{+\frac{h}{2}} \tau_{yz} dz \tag{8}$$

$$\mathbf{N} = \int_{-h/2}^{+h/2} \mathbf{E}(z) dz \bar{\varepsilon} + \int_{-h/2}^{+h/2} \mathbf{E}(z) z dz \kappa$$

$$\mathbf{M} = \int_{-h/2}^{+h/2} \mathbf{E}(z) z dz \bar{\varepsilon} + \int_{-h/2}^{+h/2} \mathbf{E}(z) z^2 dz \kappa$$

$$\mathbf{V} = (k^*) \int_{-h/2}^{+h/2} \mathbf{E}^t(z) dz \gamma \tag{9}$$

The individual components are written in following general form

$$N_1 = A_{11}\left(\frac{\partial u_1}{\partial x_1} + \frac{u_3}{R_1}\right) + A_{12}\left(\frac{\partial u_2}{\partial x_2} + \frac{u_3}{R_2}\right) + \\ + A_{16}\left(\frac{\partial u_2}{\partial x_1} + \frac{\partial u_1}{\partial x_2}\right) + B_{11}\frac{\partial^2 u_3}{\partial x_1^2} + B_{12}\frac{\partial^2 u_3}{\partial x_2^2} + \\ + B_{16}\left(2\frac{\partial^2 u_3}{\partial x_1 \partial x_2} - \frac{1}{2}\left(\frac{1}{R_1} - \frac{1}{R_2}\right)\left(\frac{\partial u_2}{\partial x_1} - \frac{\partial u_1}{\partial x_2}\right)\right) \tag{10}$$

$$N_2 = A_{21}\left(\frac{\partial u_1}{\partial x_1} + \frac{u_3}{R_1}\right) + A_{22}\left(\frac{\partial u_2}{\partial x_2} + \frac{u_3}{R_2}\right) + \\ + A_{26}\left(\frac{\partial u_2}{\partial x_1} + \frac{\partial u_1}{\partial x_2}\right) + B_{21}\frac{\partial^2 u_3}{\partial x_1^2} + B_{22}\frac{\partial^2 u_3}{\partial x_2^2} + \\ + B_{26}\left(2\frac{\partial^2 u_3}{\partial x_1 \partial x_2} - \frac{1}{2}\left(\frac{1}{R_1} - \frac{1}{R_2}\right)\left(\frac{\partial u_2}{\partial x_1} - \frac{\partial u_1}{\partial x_2}\right)\right) \tag{11}$$

$$N_6 = A_{61}\left(\frac{\partial u_1}{\partial x_1} + \frac{u_3}{R_1}\right) + A_{62}\left(\frac{\partial u_2}{\partial x_2} + \frac{u_3}{R_2}\right) + \\ + A_{66}\left(\frac{\partial u_2}{\partial x_1} + \frac{\partial u_1}{\partial x_2}\right) + B_{61}\frac{\partial^2 u_3}{\partial x_1^2} + B_{62}\frac{\partial^2 u_3}{\partial x_2^2} + \\ + B_{66}\left(2\frac{\partial^2 u_3}{\partial x_1 \partial x_2} - \frac{1}{2}\left(\frac{1}{R_1} - \frac{1}{R_2}\right)\left(\frac{\partial u_2}{\partial x_1} - \frac{\partial u_1}{\partial x_2}\right)\right) \tag{12}$$

$$M_1 = B_{11}\left(\frac{\partial u_1}{\partial x_1} + \frac{u_3}{R_1}\right) + B_{12}\left(\frac{\partial u_2}{\partial x_2} + \frac{u_3}{R_2}\right) +$$
$$+ B_{16}\left(\frac{\partial u_2}{\partial x_1} + \frac{\partial u_1}{\partial x_2}\right) + D_{11}\frac{\partial^2 u_3}{\partial x_1^2} + D_{12}\frac{\partial^2 u_3}{\partial x_2^2} +$$
$$+ D_{16}\left(2\frac{\partial^2 u_3}{\partial x_1 \partial x_2} - \frac{1}{2}\left(\frac{1}{R_1} - \frac{1}{R_2}\right)\left(\frac{\partial u_2}{\partial x_1} - \frac{\partial u_1}{\partial x_2}\right)\right)$$
(13)

$$M_2 = B_{21}\left(\frac{\partial u_1}{\partial x_1} + \frac{u_3}{R_1}\right) + B_{22}\left(\frac{\partial u_2}{\partial x_2} + \frac{u_3}{R_2}\right) +$$
$$+ B_{26}\left(\frac{\partial u_2}{\partial x_1} + \frac{\partial u_1}{\partial x_2}\right) + D_{21}\frac{\partial^2 u_3}{\partial x_1^2} + D_{22}\frac{\partial^2 u_3}{\partial x_2^2} +$$
$$+ D_{26}\left(2\frac{\partial^2 u_3}{\partial x_1 \partial x_2} - \frac{1}{2}\left(\frac{1}{R_1} - \frac{1}{R_2}\right)\left(\frac{\partial u_2}{\partial x_1} - \frac{\partial u_1}{\partial x_2}\right)\right)$$
(14)

$$M_6 = B_{61}\left(\frac{\partial u_1}{\partial x_1} + \frac{u_3}{R_1}\right) + B_{62}\left(\frac{\partial u_2}{\partial x_2} + \frac{u_3}{R_2}\right) +$$
$$+ B_{66}\left(\frac{\partial u_2}{\partial x_1} + \frac{\partial u_1}{\partial x_2}\right) + D_{61}\frac{\partial^2 u_3}{\partial x_1^2} + D_{62}\frac{\partial^2 u_3}{\partial x_2^2} +$$
$$+ D_{66}\left(2\frac{\partial^2 u_3}{\partial x_1 \partial x_2} - \frac{1}{2}\left(\frac{1}{R_1} - \frac{1}{R_2}\right)\left(\frac{\partial u_2}{\partial x_1} - \frac{\partial u_1}{\partial x_2}\right)\right)$$
(15)

$$V_1 = k_1 A_{44}\left(\frac{\partial u_3}{\partial x_1} - \frac{u_1}{R_1}\right) \quad V_2 = k_2 A_{55}\left(\frac{\partial u_3}{\partial x_2} - \frac{u_2}{R_2}\right)$$
(16)

The internal forces can be written in hypermatrix form

$$\begin{Bmatrix} N \\ M \end{Bmatrix} = \begin{bmatrix} A & B \\ B & D \end{bmatrix} \begin{Bmatrix} \bar{\varepsilon} \\ \kappa \end{Bmatrix} \qquad V = k\overline{A}\gamma$$
(17)

where N is the membrane force resultant vector, M is the moment resultant vector and V is the transverse shear force resultant vector. In addition, A, D, B denote the classical extensional stiffness matrix, bending stiffness matrix and bending-extensional coupling stiffness matrix, respectively, whereas $\overline{A}$ is the shear stiffness matrix [15,16].
The components of A, B, D, $\overline{A}$ matrix are written as

$$A = \int_{-h/2}^{+h/2} E(z)dz = \sum_{n=1}^{N}\int_{n-1_z}^{n_z} {}^n E dz = \sum_{n=1}^{N} {}^n E^n h$$

$$B = \int_{-h/2}^{+h/2} E(z)z\,dz = \sum_{n=1}^{N}\int_{n-1_z}^{n_z} {}^n E z\,dz = \sum_{n=1}^{N} {}^n E \frac{{}^n z^2 - {}^{n-1} z^2}{2}$$

$$D = \int_{-h/2}^{+h/2} E(z)z^2 dz = \sum_{n=1}^{N}\int_{n-1_z}^{n_z} {}^n E z^2 dz = \sum_{n=1}^{N} {}^n E \frac{{}^n z^3 - {}^{n-1} z^3}{3}$$

$$\overline{A} = \int_{-h/2}^{+h/2} E^t(z)dz = \sum_{n=1}^{N} {}^n E^{t\,n} h$$
(18)

III. FINITE ELEMENT ANALYSIS

The basic idea of the FEM is a discretisation of the continuous structure. The discretisation is defined by finite element mesh make up of elements nodes. The starting point for elastostatic problems is the total potential energy. In accordance with the Ritz method the approximation is used for displacement field vector by notation

$$\tilde{u}(x) = [\phi](x)v ,$$
(19)

where $\phi(x)$ is the matrix of the shape functions, that are functions of the position vector x and v is the element displacement vector.
For the stresses and strains we obtain

$$\sigma(x) = E\varepsilon(x) = ED\phi(x)v$$

$$\varepsilon(x) = Du(x) = D[\phi](x)v = B(x)v$$
(20)

The total potential energy is a function of all the nodal displacement components arranged in the element displacement vector v. The variation of the total potential energy

$$\delta\Pi = \delta v^T\left(\int_V B^T EB v\,dV - \int_V [\phi]^T p\,dV - \int_{O_q} [\phi]^T q\,dO\right)$$
(21)

leads to

$$\delta v^T\left(Kv - f_p - f_q\right) = 0$$
(22)

where p, q are volume and surface loadings, respectively and K is the symmetric stiffness matrix given by

$$K = \int_V B^T EB\,dV$$
(23)

The vectors of the volume forces and the surface forces are written by
$$f_p = \int_V [\phi]^T p\,dV$$

$$f_q = \int_{O_q} [\phi]^T q\,dO$$
(24)

If the components of δv are independent of each other, we obtain from Eq. (22) the system of linear equations

$$Kv = f$$

$$f = f_p + f_q$$
(25)

All equations considered above are valid for a single finite element and they should have an additional index E. We have the inner element energy

$$U_E = \frac{1}{2}v_E^T \int_{V_E} B^T EB\,dV v_E = \frac{1}{2}v_E^T K_E v_E$$
(26)

with the element stiffness matrix

$$K_E = \int_{V_E} B^T E B dV$$

$$E = \sum_{n=1}^{N} {}^n E$$

$${}^n E = \overline{T}^T \left({}^n \beta\right)^{(n)} E_L \overline{T}\left({}^n \beta\right) \quad (27)$$

where E is the elasticity matrix obtained with suitable transformations in two stages, firstly from the principal material directions to the element local directions and secondly to the global directions. B is the strain matrix, T is the transformation matrix with

$$\overline{T}(\alpha) = \left(T^T(\alpha)\right)^{-1} \quad (28)$$

The system stiffness matrix is also symmetric, but it is a singular matrix. After consideration of the boundary conditions of the whole system, K becomes a positive definite matrix and the system equations can be solved.

FE analysis is sensitive regarding to the strains and stresses (post-processing results) because the secondary solution converges slower than the primary solution. Quadratic elements have two basic disadvantages: the numerical effort increases and the meshing of a free-form surface is more complex because the thickness-to-curvature ratio has to be considered. Recently improvements in computing power, memory, and meshing algorithms make these elements more useful. The gain of higher shape-function approaches are better displacement, strain, and stress results. In addition, curved surfaces are mapped better because the shape functions are also used to describe the element geometry (isoparametric elements). The element descriptions are presented by Cook [17]. The quadratic shape functions of the 6-node and 8-node element (Fig. 3) are given in Equation 29 and 31, respectively [18].

The quadratic shape functions of the 6-node element have following form

$$\Phi_1 = L_1(2L_1 - 1)$$
$$\Phi_2 = L_2(2L_2 - 1)$$
$$\Phi_3 = L_3(2L_3 - 1)$$
$$\Phi_4 = 4L_1 L_2$$
$$\Phi_5 = 4L_2 L_3$$
$$\Phi_6 = 4L_3 L_1 \quad (29)$$

where

$$L_1 = 1 - \xi - \eta, \ L_2 = \xi \text{ and } L_3 = \eta. \quad (30)$$

The quadratic shape functions of the 8-node element (Fig. 3) written in dimensionless coordinates are used in this study.

$$\Phi_1 = 0.25(1-\xi)(1-\eta)(-\xi-\eta-1)$$
$$\Phi_2 = 0.25(1+\xi)(1-\eta)(\xi-\eta-1)$$
$$\Phi_3 = 0.25(1+\xi)(1+\eta)(\xi+\eta-1)$$
$$\Phi_4 = 0.25(1-\xi)(1+\eta)(-\xi+\eta-1)$$
$$\Phi_5 = 0.5(1-\xi^2)(1-\eta)$$
$$\Phi_6 = 0.5(1+\xi)(1-\eta^2)$$
$$\Phi_7 = 0.5(1-\xi^2)(1+\eta)$$
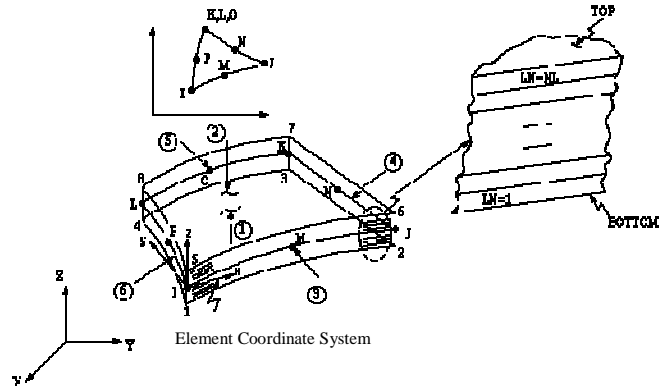$$\Phi_8 = 0.5(1-\xi)(1-\eta^2) \quad (31)$$

Fig. 3 SHELL99 linear layered structural shell [19]

IV. MODAL ANALYSIS

The main objective of any modal analysis is to make sure the structure is not subject to resonant frequency under the range of operation. Natural frequency is the frequency at which the structure vibrates if the forcing function is identically zero. The lowest natural frequency is often referred to as the fundamental frequency, which is the most important parameter for design engineers as many of the systems are designed to operate below it.

There are several mode extraction methods. Each method has its own advantages and disadvantages. The method that is used in the present work is the subspace method. Modal analysis is the preliminary step of a dynamic transient analysis.

For the finite element analysis, if the damping is neglected, the equation of motion of the structure for free vibration can be written as

$$M_D \ddot{v}(t) + K v(t) = 0 \quad (32)$$

The particular solutions are

$$v(t) = v_j^0 \sin(\omega_j t) \quad \text{and} \quad v(t) = v_j^0 \cos(\omega_j t) \quad (33)$$

Than we get

$$\left(K - \omega_j^2 M_D\right) v_j^0 = 0 \quad (34)$$

where K is stiffness matrix, v_j^0 is mode shape vector of mode j, ω_j is the natural circular frequency, ω_j^2 is the eigenvalue and M_D is the mass matrix.

After modification of (34) we get

$$M_D^{-1}\left(K - \omega_j^2 M_D\right) v_j^0 = M_D^{-1} 0 \quad D^{-1} - \omega_j^2 E_D v_j^0 = 0 \quad (35)$$

where

$$D^{-1} = M_D^{-1} K = K_r \quad (36)$$

The equation (35) means the eigenvalue problem, where ω_j^2 are eigenvalues of the matrix D^{-1} and v_j^0 are natural modes of vibration.

V. EXAMPLE AND RESULTS

For this study, a double curved laminated shell with the following dimensions is selected:
$a = b = 0.8$ m, $R_1 = R_2 = 2.4$ m , $h = 8$mm.
An unidirectional fiber reinforced composite laminate layer consists of isotropic fibers:
$E_f = 270$ GPa, $v_f = 0.3$, $\rho_f = 1800$ kg·m^{-3}

and isotropic matrix:
$E_m = 5$ GPa, $v_m = 0.3$, $\rho_m = 1500$ kg·m^{-3}.

The fiber volume fraction $\xi = 0.4$ and fiber diameter $d = 9\,\mu$m.

Most fiber reinforced composites have a random arrangement of the fibers at the micro-scale. A random microstructure results in transversely isotropic properties at the meso-scale. A simpler alternative is to assume that the random microstructure is well approximated by the hexagonal microstructure (Fig. 4).
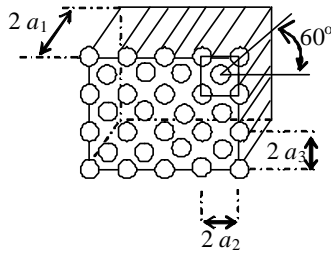
Fig. 4 Hexagonal microstructure model

An analysis of microstructure yields a transversely isotropic stiffness tensor

$$
\begin{Bmatrix} \bar{\sigma}_1 \\ \bar{\sigma}_2 \\ \bar{\sigma}_3 \\ \bar{\sigma}_4 \\ \bar{\sigma}_5 \\ \bar{\sigma}_6 \end{Bmatrix} = \begin{bmatrix} C_{11} & C_{12} & C_{12} & 0 & 0 & 0 \\ C_{12} & C_{22} & C_{23} & 0 & 0 & 0 \\ C_{12} & C_{23} & C_{22} & 0 & 0 & 0 \\ 0 & 0 & 0 & \frac{1}{2}(C_{22} - C_{23}) & 0 & 0 \\ 0 & 0 & 0 & 0 & C_{66} & 0 \\ 0 & 0 & 0 & 0 & 0 & C_{66} \end{bmatrix} \begin{Bmatrix} \bar{\varepsilon}_1 \\ \bar{\varepsilon}_2 \\ \bar{\varepsilon}_3 \\ \bar{\gamma}_4 \\ \bar{\gamma}_5 \\ \bar{\gamma}_6 \end{Bmatrix}. \quad (37)
$$

where the 1-axis aligned with the fiber direction and an over-bar indicates the average computed over the volume of the RVE.
Coefficients of the stiffness tensor are written in the Tables 1-4.

TABLE I
COEFFICIENTS OF THE FIRST COLUMN OF STIFFNESS TENSOR

V [μm^3]	C_{11} [MPa]	C_{21} [MPa]	C_{31} [MPa]
134.705	114277.5	5463.704	5463.3129

TABLE II
COEFFICIENTS OF THE SECOND COLUMN OF STIFFNESS TENSOR

V [μm^3]	C_{12} [MPa]	C_{22} [MPa]	C_{32} [MPa]
134.705	5464.704	13006.51	5209.964

TABLE III
COEFFICIENTS OF THE THIRD COLUMN OF STIFFNESS TENSOR

V [μm^3]	C_{13} [MPa]	C_{23} [MPa]	C_{33} [MPa]
134.705	5463.073	5209.964	13006.08

TABLE IV
COEFFICIENT OF THE SIXTH COLUMN OF STIFFNESS TENSOR

V [μm^3]	C_{66} [MPa]
1074.64	2166.161

TABLE V
SUMARY OF RESULTS OF HEXAGONAL NUMERICAL MODEL

$E_1 = E_3$ [GPa]	110.999
E_2 [GPa]	10.824
$v_{12} = v_{13}$	0.3
v_{23}	0.388
$G_{12} = G_{13}$ [GPa]	4.79
G_{23} [GPa]	3.899

Four-layer cross-ply [0/90/90/0], [0/90/0/90] and angle-ply [45/-45/-45/45], [45/-45/45/-45] laminates are analysed to study the effect of symmetry to change the resonant frequencies (Tabs. 6).
From the Tables 6 can be seen, the frequencies in the case of angle-ply laminate are higher than in the case of cross-ply laminate. The frequencies in the case of symmetric layup are the same than in the case of anti-symmetric layup for both kinds of laminates.

TABLES VI
INFLUENCE OF FIBER ORIENTATION ON FREQUENCIES

Frequencies	1st	2nd	3rd
[0/90/90/0]	6.472	6.923	7.599
[0/90/0/90]	6.472	6.923	7.599
[45/-45/-45/45]	8.145	8.234	8.663
[45/-45/45/-45]	8.145	8.234	8.663

Frequencies	4th	5th	6th
[0/90/90/0]	7.766	7.894	8.064
[0/90/0/90]	7.766	7.894	8.064
[45/-45/-45/45]	8.796	8.904	8.986
[45/-45/45/-45]	8.796	8.904	8.986

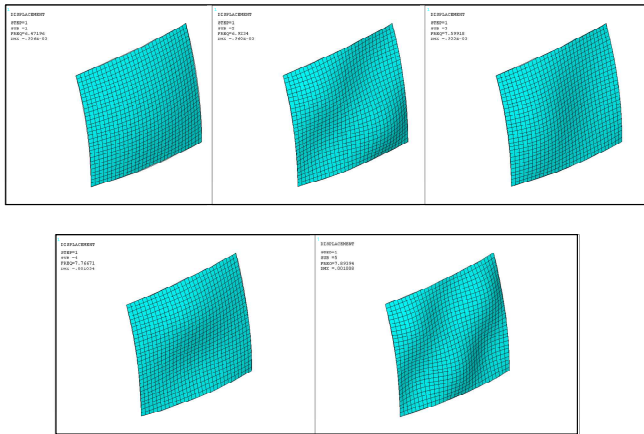| Frequencies	7th	8th	9th
[0/90/90/0]	8.499	9.274	9.613
[0/90/0/90]	8.499	9.274	9.613
[45/-45/-45/45]	10.532	10.630	11.009
[45/-45/45/-45]	10.532	10.630	11.009

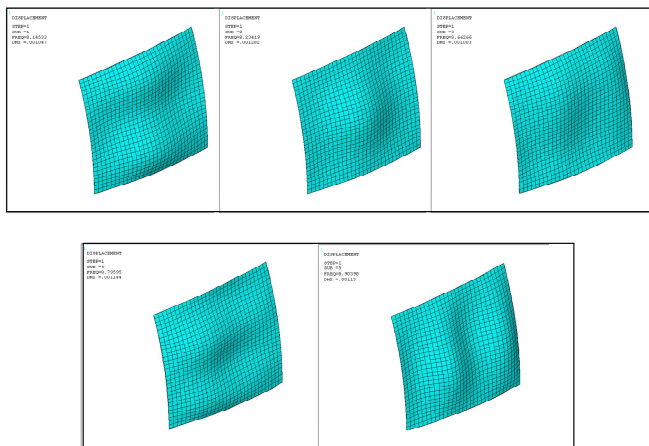Fig. 5 The first five natural modes of double curved laminated shell [0/90/90/0]

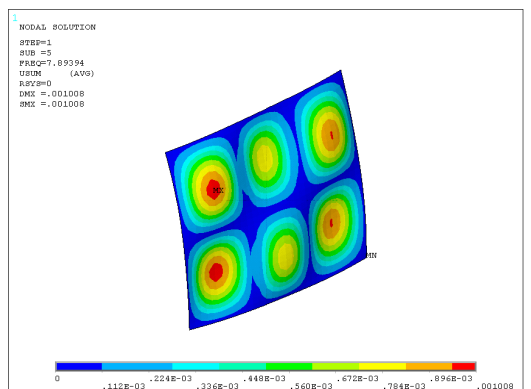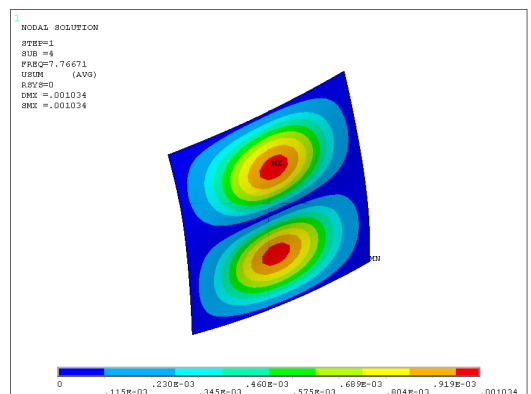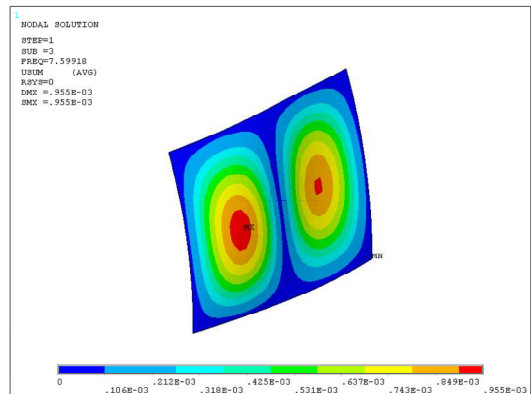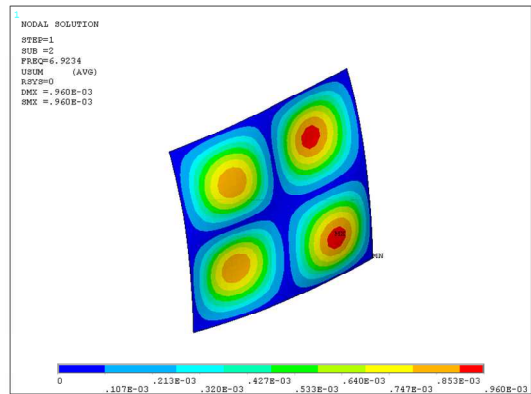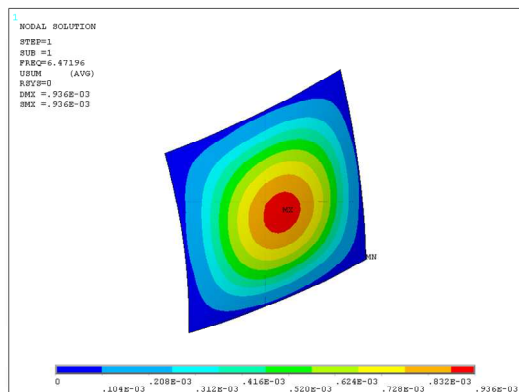Fig. 6 The first five natural modes of double curved laminated shell [45/-45/-45/45]

Fig. 7 Displacements of the first five natural modes of double curved [0/90/90/0] laminated shell, respectively
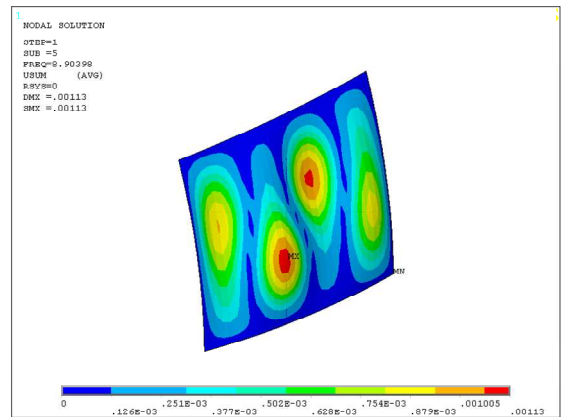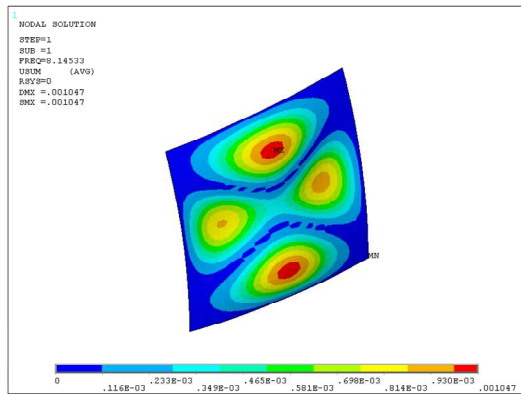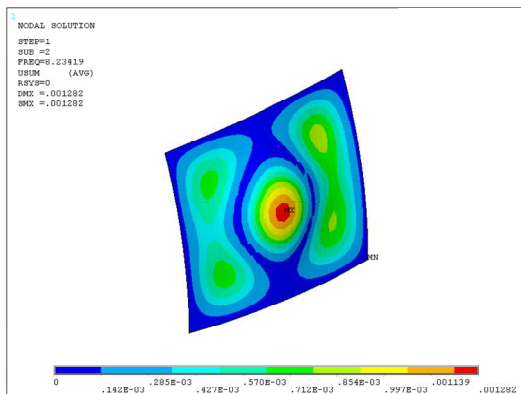
Fig. 8 Displacements of the first five natural modes of double curved [45/-45/-45/45] laminated shell, respectively

From the Figs. 5-8 can be seen, the natural modes in the case of angle-ply laminate are more complicated than in the case of cross-ply laminate.

TABLE VII
INFLUENCE OF B/H RATIO TO FUNDAMENTAL FREQUENCY

b/h ratio	[0/90/90/0]	[45/-45/-45/45]
100	6.47196	8.14533
200	6.45032	7.54193
400	6.44501	7.14498
800	6.44344	6.88707
1000	6.44301	6.83161
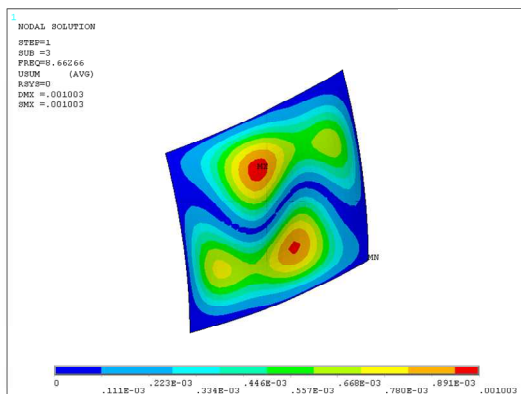
In the Table 7 the width-to-thickness ratio is analysed. As can be seen from Table 7, as b/h increases, the fundamental frequency decreased. Degrease of fundamental frequency is more evident for [45/-45/-45/45] laminate than for [0/90/90/0] laminate.

TABLE VIII
INFLUENCE OF FIBER ORIENTATION TO FUNDAMENTAL FREQUENCY

α	$[\alpha/-\alpha/-\alpha/\alpha]$	$[\alpha/-\alpha/\alpha/-\alpha]$
0	5.65538	5.65538
15	5.91056	5.91056
30	6.63442	6.63442
45	8.14533	8.14533
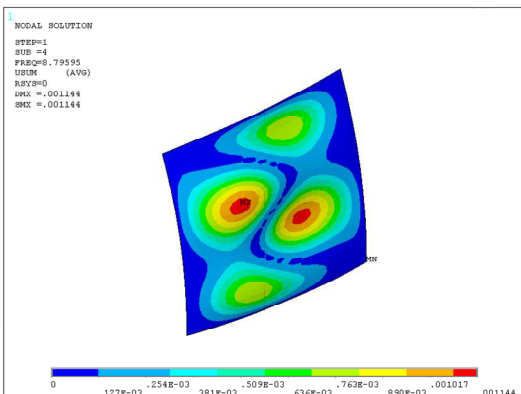
Four-layer symmetric $[\alpha/-\alpha/-\alpha/\alpha]$ and anti-symmetric $[\alpha/-\alpha/\alpha/-\alpha]$ laminates with the angle of fibre orientation varying from $0^o - 45^o$ with $b/h = 100$ are analysed. As can be seen from Table 8, an increase of fibre orientation angle leads to an increase in the frequency of vibration. Also as it was written, the frequency in the case of symmetric layup is the same as in the case of anti-symmetric layup of laminates.

VI. DISCUSSION AND CONCLUSION

The material properties of unidirectional fiber reinforced composite are done by the numerical homogenization [20] of

unidirectional lamina (Table 5). Within the numerical homogenization, the hexagonal microstructure model was assumed in RVE. The numerical homogenization was done by using the Finite Element Method [21] in the program ANSYS.

In the paper, mode-frequency analysis of laminated double curved shell using a finite element model, based on first-order shear deformation theory is presented.

The frequencies in the case of angle-ply laminate are higher than in the case of cross-ply laminate. The frequencies in the case of symmetric layup are the same than in the case of anti-symmetric layup for both kinds of laminates. The natural modes in the case of angle-ply laminate are more complicated than in the case of cross-ply laminate. As width-to-thickness ratio b/h increases, the fundamental frequency decreased. Degrease of fundamental frequency is more evident for [45/-45/-45/45] laminate than for [0/90/90/0] laminate. An increase of fibre orientation angle leads to an increase in the fundamental frequency of vibration.

REFERENCES

[1] M. Žmindák, P. Pastorek, "Finite Element Analysis of Cohesion between Reinforced Concrete Beam and Polymer Lamella Reinforced by Carbon Fibers", *Procedia Engineering*, 177, 582-589, 2017.

[2] M. Miháliková, A. Lišková, "Dynamic characteristics of automotive steel sheets", *Metalurgija*, 55(4), 753-756, 2016.

[3] E. Kormaníková. K. Kotrasová, "Delamination of laminate plate under tearing load mode", *MATEC Web of Conferences*, 107,00049, 2017.

[4] 4. P.M. Wung, "Laminated composite structures by continuumbased shell elements with transverse deformation", *Computers and Structures*, 62(6), 1073–1090, 1996.

[5] J. Whitney and N. Pagano, "Shear deformation in heterogeneous anisotropic plates", *Journal of Applied Mechanics*, 37,1031–1040, 1970.

[6] S.B. Dong and F.K.W. Tso, "On a laminated orthotropic shell theory including transverse shear deformation", *ASME Journal of Applied Mechanics*, 39,1091–1096, 1972.

[7] E. Kormaníková. K. Kotrasová, "Laminate circular cylindrical shell", *MATEC Web of Conferences*, 125,04010, 2017.

[8] E. Kormaníková. K. Kotrasová, "Resonant frequencies and mode shapes of rectangular sandwich plate", *Chemicke Listy*, 105(16),535-538, 2011.

[9] A. H. Sofiyev, D. Hui, V. C. Haciyev, H. Erdem, G. Q. Yuan, E. Schnack, V. Guldal, "The nonlinear vibration of orthotropic functionally graded cylindrical shells surrounded by an elastic foundation within first order shear deformation theory", *Composites Part B: Engineering*, 116, 170-185, 2017.

[10] S. Brischetto, "Exact three-dimensional static analysis of single- and multi-layered plates and shells", *Composites Part B: Engineering*, 119, 230-252, 2017.

[11] F. Tornabene, A. Ceruti, "Mixed Static and Dynamic Optimization of Four-Parameter Functionally Graded Completely Doubly Curved and Degenerate Shells and Panels Using GDQ Method", *Mathematical Problems in Engineering* 1, 1-33, 2013.

[12] K. Kotrasová, E. Kormaníková, "A case study on seismic behavior of rectangular tanks considering fluid - structure interaction", *International Journal of Mechanics*, 10, 242-252, 2016.

[13] M. Amabili, J.N. Reddy, "A new non-linear higher-order shear deformation theory for large-amplitude vibrations of laminated doubly curved shells", *International Journal of Non-Linear Mechanics*, 45, 409–418, 2009.

[14] R. Roos, *Model for interlaminar normal stresses in doubly curved laminates*, Dissertation, Swiss Federal Institute of Technology, Zurich, 2008.

[15] U. Topal, "Frequency Optimization of Laminated Composite Spherical Shells", *Science and Engineering of Composite Materials*, 19,381-386, 2012.

[16] M. Krejsa, J. Brozovsky, D. Mikolasek, R. Halama, J. Kozak, "Numerical modeling of steel fillet welded joint", *Advances in Engineering Software*, 117, 59-69, 2018.

[17] R.D. Cook, D.S. Malkus, M.E. Plesha, and R.J. Witt, *Concepts and applications of finite element analysis*. John Wiley and Sons, fourth edition, 2002.

[18] J.N. Reddy, *Mechanics of Laminated Composite Plates and Shells: Theory and Analysis*, second ed., CRC Press, Boca Raton, FL, USA, 2004.

[19] http://www.ansys.stuba.sk/html/elem_55/chapter4/ES4-99.htm

[20] H. Massow, W. Becker, "Homogenization of Folded Sandwich Core Structure", *International Journal of Mechanics*, vol. 11, pp. 25–33, 2017.

[21] O. Sucharda, J. Vasek, and J. Kubosek, "Elastic-plastic calculation of a steel beam by the finite element method," *International Journal of Mechanics*, vol. 9, pp. 228–235, 2015.

E. Kormanikova is associate professor of Structural and Transportation Engineering in Faculty of Civil Engineering of Technical University of Košice, Slovakia. She is member of Central Committee of the Slovak Society for Mechanics, Slovak Academy of Science, member of the Central European Association for Computational Mechanics, member of the Standard Committee 15: Actions on Structures.

Her research field: Design and optimization of structural elements and structures made of composite materials, Modeling of delamination of composite materials, Statics and dynamics of the civil engineering structures.